Acta Crystallographica Section B
Structural Science
ISSN 0108-7681

$Li_{3+\delta}V_6O_{13}$: a short-range-ordered lithium insertion mechanism

Jonas Höwing, Torbjörn Gustafsson* and John O. Thomas

Department of Materials Chemistry, Ångström Laboratory, Uppsala University, Box 538, SE-751 21 Uppsala, Sweden

Correspondence e-mail: tgn@mkem.uu.se

Received 20 February 2004
Accepted 1 June 2004

The structures of $Li_3V_6O_{13}$ and $Li_{3+\delta}V_6O_{13}$, $\delta \simeq 0.3$, have been determined by single-crystal X-ray diffraction. Both compounds have the space group $C2/m$, with very similar cell parameters. In $Li_3V_6O_{13}$, the Li atoms are found in the Wyckoff positions 4(*i*) and 2(*b*) with multiplicities of four and two, respectively. Since $Li_3V_6O_{13}$ exhibits no superstructure reflections, it is concluded that $Li_3V_6O_{13}$ contains one disordered lithium ion in an otherwise ordered centrosymmetric structure. On inserting more lithium into the structure, the $Li_{3+\delta}V_6O_{13}$ phase is formed with the homogeneity range $0 < \delta < 1$. It is concluded that the site for the extra inserted lithium ion is closely coupled to the position of the disordered lithium ion in $Li_3V_6O_{13}$. A mechanism for this behaviour and for the further formation of the $Li_6V_6O_{13}$ end-phase in the $Li_xV_6O_{13}$ system is proposed.

1. Introduction

The lithium-ion battery is fast becoming a common feature of today's society. It is the dominant power source in laptop computers and cell phones and, since its power capability is steadily increasing, it is also beginning to replace the nickel metal hydride (NiMH) battery for cordless power-tools. Commercially available batteries often involve $LiCoO_2$ or $Li(Co,Ni)O_2$ as the cathode, LiTFSI (lithium trifluoromethanesulfonylimide) dissolved in some organic carbonate as the electrolyte, and a graphite anode.

Although V_6O_{13} has been researched extensively over the years as a cathode material for lithium polymer batteries, its lack of lithium in its stable form means that V_6O_{13} itself is today really only of interest as a model compound for the study of lithium-insertion mechanisms. The structure of V_6O_{13}, comprising corner- and edge-sharing distorted VO_6-octahedra arranged in alternating single and double layers, was first solved as $V_{12}O_{26}$ by Aebi (1948) and later refined by Wilhelmi *et al.* (1971) in the monoclinic space group $C2/m$. The structure can host as many as six lithium ions per formula unit, giving it a theoretical capacity of 314 mAh g^{-1}. During discharge, several stoichiometric phases, $Li_xV_6O_{13}$ (x = 2/3, 1, 2, 3 and 6), are formed. The first four of these structures have been determined using single-crystal X-ray diffraction; the phases $Li_{2/3}V_6O_{13}$ and LiV_6O_{13} form superstructures of the V_6O_{13} structure involving unit-cell volume tripling and doubling, respectively (Björk *et al.*, 2001). The original V_6O_{13} unit-cell is again found for $Li_2V_6O_{13}$ (Bergström *et al.*, 1997). In all these structures, the lithium ion is situated close to the single layer, fivefold coordinated in a square pyramidal arrangement by O atoms. In $Li_3V_6O_{13}$, a total rearrangement of the lithium ions occurs as they move into the double layer (Bergström *et al.*, 1998), while newly inserted lithium ions are incorporated into

the single layer. The new lithium ion in the single layer is disordered and randomly distributed above and below the *ab* plane.

The discharge curve for V_6O_{13} *versus* Li/Li^+ is given in Fig. 1. The different stoichiometric phases and their corresponding potentials *versus* Li metal are indicated. The shape of such a discharge curve (potential *versus* charge) depends on the lithium-insertion mechanism taking place. If a solid solution is formed, the discharge curve will slope gradually, but if the material passes through a series of discrete stoichiometric phases each new phase formed will correspond to an abrupt drop in potential; in a two-phase region, the potential will be quite constant (Ceder & Aydinol, 1998). With the superstructure formation reported by Björk *et al.* (2001) in mind, it is reasonable to assume that the apparently disordered lithium ion in $Li_3V_6O_{13}$ is merely an artefact of superstructure formation. This structure was therefore reinvestigated using a diffractometer equipped with an area detector, since weak reflections arising from possible superstructure formation are more easily detected with such a system. As can be seen in the discharge curve (Fig. 1), a large potential drop occurs after $Li_3V_6O_{13}$; to our knowledge, this region has not been investigated earlier. This drop can originate from the formation of either a new stoichiometric phase or of a hitherto unobserved solid solution system. In this work, single crystals of V_6O_{13} have been electrochemically lithiated to both 2.45 and 2.30 V. The structures have been determined using single-crystal X-ray diffraction data.

2. Experimental

2.1. Sample preparation

Single crystals of V_6O_{13} were grown using the Chemical Vapour Transport (CVT) technique described by Saeki *et al.* (1973). V_6O_{13} powder was synthesized by the decomposition of NH_4VO_3, as described by Lampe-Önnerud & Thomas (1995). Powder cathodes were prepared by ball milling together the as-synthesized V_6O_{13}, carbon black and EPDM (ethylene propylene diene copolymer), dissolved in cyclohexane, in a 80:15:5 mass % ratio. The cathode slurry was then spread onto an aluminium foil using a wire bar and cathodes with a 2.0 cm diameter were punched out. A small point on the cathodes was scraped clean of powder cathode and five single crystals with suitable dimensions (maximum 0.1 mm) were placed on the exposed aluminium. A slurry of carbon black and EPDM (4:1 mass ratio) dissolved in cyclohexane was then dropped onto the crystals. Great care was taken to ensure that the crystals were not washed away but remained completely immersed in the carbon black.

The cathodes thus prepared were then transferred to a glove-box with an Ar atmosphere (O_2, H_2O < 5 p.p.m.) and vacuum-dried overnight at 393 K. They were then incorporated into a test cell of 'coffee-bag' type (Gustafsson *et al.*, 1992). The electrolyte used was 1 *M* $LiPF_6$ in EC/DMC (ethylene and dimethyl carbonate, respectively) in a 2:1 by volume mixture. The cells were connected to a Digatron MBT testing unit with BTS-600 software and discharged galvanostatically to 2.45 V, corresponding to the composition $Li_3V_6O_{13}$. The batteries were then allowed to equilibrate at this potential for 2 months. One of the cells was then dismantled and the crystals recovered, while the other was discharged to 2.30 V (approximate composition $Li_{3.4}V_6O_{13}$) and left to equilibrate for 1 month. This cell was finally dismantled and the crystals recovered.

Many of the crystals discharged in the battery to 2.45 V had shattered, but one quite large crystal could be extracted. It was mounted on a glass needle with epoxy glue. In the battery discharged to 2.30 V, all crystals shattered during the electrochemical treatment; the larger pieces were very fragile and split readily into thin needles. One piece with the approximate dimensions $0.05 \times 0.02 \times 0.01$ mm^3 was attached to a glass needle with epoxy glue, and then transferred into the glove-box and vacuum packed for transport to the synchrotron.

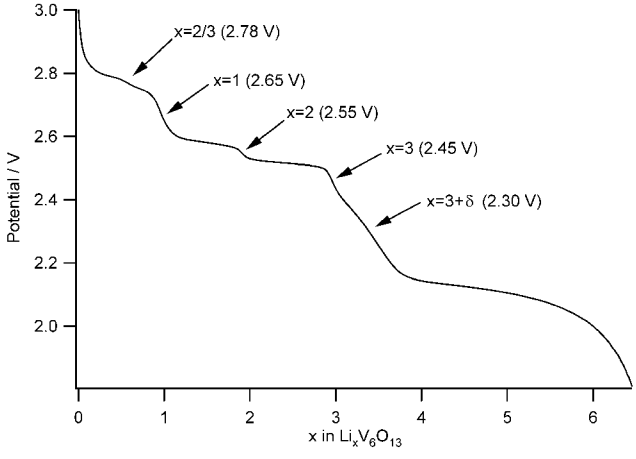

Figure 1
The discharge curve for V_6O_{13} *versus* Li/Li^+. The compositions of the different lithiated phases formed and their corresponding cell potentials are marked.

2.2. Diffraction experiments

A Bruker SMART Apex diffractometer equipped with a CCD detector using Ag $K\bar{\alpha}$ radiation (λ = 0.56086 Å) was used for the crystal discharged to 2.45 V. The detector was positioned at $2\theta = 28°$, covering the range $2\theta = 0$–$56°$. The data collection was performed using 0.2° ω scans with 30 s exposure times and 1024 × 1024 pixel detector resolution.

The crystal discharged to 2.30 V was studied on the synchrotron beamline I711 at MAX-lab, Lund, Sweden (Cerenius *et al.*, 2000). Data were collected using a Bruker Smart 1000 CCD detector set at 512 × 512 pixel resolution; λ = 0.872 Å. Data were collected up to *ca* $2\theta = 100°$. To optimize the benefits of the higher intensity of a synchrotron beam, a special data-collection strategy was used. A complete dataset was first collected using maximum beam intensity. In this dataset, the detector was saturated for a number of strong low-angle reflections. A second dataset was thereafter collected with the beam attenuated to such an extent that the strongest

Table 1
Experimental details.

	$Li_3V_6O_{13}$	$Li_{3+\delta}V_6O_{13}$
Crystal data		
Chemical formula	$Li_3V_6O_{13}$	$Li_{3.25}V_6O_{13}$
M_r	534.5	536.2
Cell setting, space group	Monoclinic, *C*2/*m*	Monoclinic, *C*2/*m*
a, *b*, *c* (Å)	11.792 (1), 3.9214 (4), 10.189 (1)	11.7236 (6), 3.9155 (2), 10.1521 (5)
β (°)	100.596 (2)	100.592 (2)
V (Å^3)	463.12 (8)	458.08 (4)
Z	2	2
D_x (Mg m^{-3})	3.831 (1)	3.886 (1)
Radiation type	Ag $K\bar{\alpha}$	Synchrotron
No. of reflections for cell parameters	855	594
θ range (°)	5.5–54.7	9.2–63.8
μ (mm^{-1})	3.01	10.35
Temperature (K)	295	295
Crystal form, colour	Brick, black	Shard, black
Crystal size (mm)	0.20 × 0.14 × 0.04	0.05 × 0.02 × 0.01
Data collection		
Diffractometer	CCD area detector	CCD area detector
Data collection method	ω scans	ω scans
Absorption correction	Empirical (using intensity measurements)	Empirical (using intensity measurements)
No. of measured, independent and observed reflections	2830, 1179, 1179	5374, 1372, 1365
Criterion for observed reflections	$I > -15\sigma(I)$	$I > -15\sigma(I)$
R_{int}	0.027	0.040
θ_{max} (°)	28.2	50.6
Range of *h*, *k*, *l*	$-18 \Rightarrow h \Rightarrow 15$ $-5 \Rightarrow k \Rightarrow 6$ $-16 \Rightarrow l \Rightarrow 16$	$-15 \Rightarrow h \Rightarrow 20$ $-4 \Rightarrow k \Rightarrow 6$ $-17 \Rightarrow l \Rightarrow 14$
Refinement		
Refinement on	F^2	F^2
$R[F^2 > -15\sigma(F^2)]$, $wR(F^2)$, *S*	0.057, 0.059, 2.09	0.029, 0.048, 3.24
No. of reflections	1179	1365
No. of parameters	69	75
Weighting scheme	$w = 1/\sigma^2(I)$	$w = 1/\sigma^2(I)$
$(\Delta/\sigma)_{max}$	0.028	0.005
$\Delta\rho_{max}$, $\Delta\rho_{min}$ (e Å^{-3})	2.14, −1.30	1.34, −1.18

Computer programs used: *SMART* (Bruker, 2003), *SAINT*+ (Bruker, 2003), *JANA*2000 (Petricek & Dusek, 2000), *Diamond*, Version 2.1c (Berghoff, 1996).

low-angle reflection did not saturate the detector. The datasets were then combined using appropriate scaling.

For both diffraction experiments, the orientation matrices used to integrate the data were determined using *SMART* (Bruker, 2003). Data reduction, integration and cell refinement were performed using the *SAINT*+ program package (Bruker, 2003). The datasets were corrected for absorption in the crystal and mounting materials using *SADABS* (Bruker, 2003). Scaling and merging of the high- and low-intensity datasets from the synchrotron measurements, space-group determination and preparation of structure factor files were performed using *XPREP* (Bruker, 2003).

3. Refinements

*JANA*2000 (Petricek & Dusek, 2000) was used for structure refinements, calculating geometries and preparing the CIFs. The input structure for both refinements was that refined by Bergström *et al.* (1998).

3.1. $Li_3V_6O_{13}$

Surprisingly, no superstructure reflections were detected. The possible space-group assignments were *C*2/*m*, *C*2 and *Cm*; R_{int} = 0.027, 0.026 and 0.026, respectively. The structure was first refined in the centrosymmetric space group *C*2/*m*. No problems were encountered during the refinements, except for the disordered lithium ion situated on the inversion centre in the single layer. In an attempt to resolve the disorder, the space-group symmetry was lowered to *Cm*. In this space group the correlation between the formerly symmetry-related atoms was huge (> 0.97). The positional and displacement parameters of all such atoms were coupled through a centre of symmetry. In this way, the disordered lithium ion in the single layer could be refined as non-centrosymmetric in an otherwise centrosymmetric environment. Despite this, no improvement could be seen in the model. An attempt to refine the lithium ion in two different positions, slightly above and slightly below the single layer (Bergström *et al.*, 1998), with coupled occupancy factors did not improve the model and resulted in an equal distribution of lithium ions on either side of the single layer. When the occupancies of the two Li2 sites were decoupled, an equal distribution above and below the single layer was achieved with the total occupancy of the sites adding up to full occupancy. The structure was therefore refined in *C*2/*m*, with the lithium ion fixed at the inversion centre. The refinements were based on F^2 and used an averaged dataset. The condition for observed reflections was $I > -15\sigma$. In the final refinement cycles 4 reflections with $\Delta > 20\sigma$ ($\Delta = F_{obs} - F_{calc}$) were omitted from the refinements. The final agreement factor was $wR(F^2)$ = 0.059 with a goodness-of-fit (*S*) of 2.1. It should be noted that all atoms in this structure are situated on a mirror plane.

3.2. $Li_{3+\delta}V_6O_{13}$

No superstructure reflections were detected for this compound either. The possible space groups were *C*2/*m*, *C*2 and *Cm*; R_{int} = 0.040, 0.039 and 0.040, respectively. The structure was first refined in *C*2/*m*. The refinements converged

and only the lithium ion situated across the inversion centre in the single layer showed any anomaly (as in the $Li_3V_6O_{13}$ refinements). An extra lithium site was located in the difference-Fourier synthesis, between the V1 and V2 octahedra. If this site were fully occupied, the composition of the cathode would be $Li_5V_6O_{13}$; it can therefore only be partially occupied at the potential to which the battery was discharged. To refine the occupancy of this atom (Li3), U_{iso}(Li3) was constrained to follow U_{iso}(Li1). This was reasonable, since the oxygen coordination around Li3 strongly resembles that around Li1. This gave an Li3 site occupancy of 0.061 (7), resulting in the composition $Li_{3.24}V_6O_{13}$. The occupancy and displacement parameters of Li3 were then fixed to these values during the final refinement cycles.

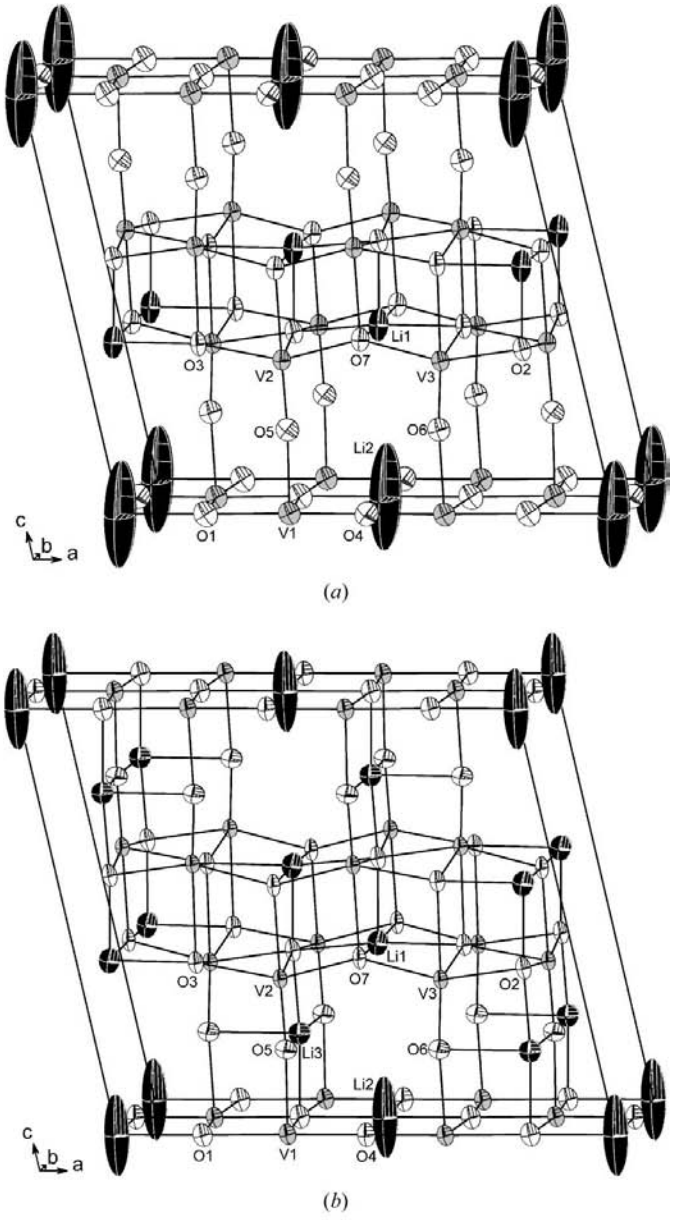

Figure 2
The structures of (*a*) $Li_3V_6O_{13}$ and (*b*) $Li_{3.24}V_6O_{13}$. The white, grey and black atoms are oxygen, vanadium and lithium, respectively. The Li2 displacement ellipsoid describes two equivalent sites above and below an inversion centre, and their partial overlap. Displacement ellipsoids are drawn at the 90% probability level.

Table 2
Selected bond lengths (Å).

	$Li_3V_6O_{13}$	$Li_{3+\delta}V_6O_{13}$
V2—O1^{i}	2.003 (3)	1.998 (1)
V1—O1^{ii}	1.9696 (3)	1.9643 (1)
V1—O1^{iii}	1.9696 (3)	1.9643 (1)
V1—O4	1.8529 (7)	1.8518 (3)
V1—O5	1.995 (2)	1.986 (2)
V1—O6^{iv}	2.025 (2)	2.012 (2)
V2—O2^{v}	1.9823 (4)	1.9777 (2)
V2—O2^{vi}	1.9823 (4)	1.9777 (2)
V2—O3	2.011 (3)	1.998 (1)
V2—O5	1.661 (2)	1.661 (2)
V2—O7	1.963 (2)	1.948 (1)
V2—O7^{vii}	2.191 (2)	2.182 (2)
V3—O2	1.983 (3)	1.976 (1)
V3—O3^{viii}	2.0072 (5)	2.0024 (3)
V3—O3^{ix}	2.0072 (5)	2.0024 (3)
V3—O3^{vii}	2.312 (2)	2.306 (2)
V3—O6	1.641 (2)	1.640 (2)
V3—O7	1.957 (3)	1.949 (1)
Li1—O2^{vi}	2.050 (7)	2.022 (4)
Li1—O2^{x}	1.994 (6)	1.988 (5)
Li1—O3^{ix}	2.022 (7)	2.018 (4)
Li1—O7	1.9615 (2)	1.9584 (1)
Li1—O7^{xi}	1.9615 (2)	1.9584 (1)
Li2—O1^{xii}	2.040 (3)	2.011 (1)
Li2—O1^{iii}	2.040 (3)	2.011 (1)
Li2—O4	1.9607 (2)	1.958 (1)
Li2—O4^{xi}	1.9607 (2)	1.958 (1)
Li3—O1^{vii}	–	1.96 (3)
Li3—O2	–	1.94 (4)
Li3—O5^{viii}	–	1.961 (2)
Li3—O5^{ix}	–	1.961 (2)
Li3—O6	–	2.14 (3)

Symmetry codes: (i) $-x, -y, -1-z$; (ii) $\frac{1}{2}-x, -\frac{1}{2}-y, 1-z$; (iii) $\frac{1}{2}-x, \frac{1}{2}-y, 1-z$; (iv) $1-x, -y, -z$; (v) $-\frac{1}{2}-x, -\frac{1}{2}-y, -z$; (vi) $-\frac{1}{2}-x, \frac{1}{2}-y, -z$; (vii) $1-x, -y, 1-z$; (viii) $\frac{1}{2}-x, -\frac{1}{2}-y, -z$; (ix) $\frac{1}{2}-x, \frac{1}{2}-y, -z$; (x) $\frac{3}{2}-x, \frac{1}{2}-y, 1-z$; (xi) $-x, 1-y, -z$; (xii) $\frac{1}{2}-x, \frac{1}{2}-y, -1-z$.

Refinement in the centrosymmetric space group *C*2/*m* gives an equal distribution of Li3 in the upper and lower part of the unit cell. The structure was therefore also refined in *Cm*, thus allowing Li3 to choose between the two different sites. Since correlation between the former symmetry-related atoms in the structure was large for many of these atoms (> 0.97), they were coupled centrosymmetrically. The occupancies of the two Li3 sites were also coupled, with the total occupancy held constant and the structure refined. This resulted in an equal occupancy of the two sites. Refinements were also performed in which Li2 was treated as described for the Li_3V_6O refinements above, in combination with the treatment of Li3. This again resulted in an equal occupancy of both the Li2 and Li3 sites.

It was thus concluded that the structure is really centrosymmetric and the final refinements were performed in the space group *C*2/*m*. All refinements were performed on F^2 using an averaged dataset with $I < -15\sigma$ as the cut-off value for unobserved reflections. Six reflections with $\Delta > 20\sigma$ were

omitted from the refinements. The final agreement factor, $wR(F^2)$, was 0.048 with a goodness-of-fit (S) of 3.25. All the atoms are again situated on a mirror plane in the structure.

4. Results and discussion

Cell parameters and final agreement factors for both structures are presented in Table 1. The refined structures for $Li_3V_6O_{13}$ and $Li_{3.24}V_6O_{13}$ are shown in Figs. 2(*a*) and 2(*b*). Atomic coordinates and equivalent isotropic displacement parameters have been deposited.[1] Selected V—O and Li—O distances for both structures are shown in Table 2. As can be seen in Table 1, the *a*, *b* and *c* axes of $Li_{3.24}V_6O_{13}$ are 0.6, 0.2 and 0.4%, respectively, shorter than in $Li_3V_6O_{13}$.

4.1. Structural aspects of $Li_3V_6O_{13}$ and $Li_{3+\delta}V_6O_{13}$

The results from the structure refinement of $Li_3V_6O_{13}$ are in good agreement with those reported previously by Bergström *et al.* (1998). The V—O bond lengths are all within three standard deviations of those reported earlier. The results from the different attempts to refine Li2 non-centrosymmetrically in a centrosymmetric environment, together with the absence of superstructure reflections, show that Li2 is disordered in an otherwise ordered structure; all previously determined $Li_xV_6O_{13}$ phases have been ordered. The formation of a superstructure has been interpreted as being triggered by the local distortion caused by the insertion of the first lithium ion. Also, in all earlier determined $Li_xV_6O_{13}$ structures, lithium has been fivefold coordinated by O atoms in a square-planar pyramidal arrangement. In $Li_3V_6O_{13}$, Li1 has this same coordination, while Li2 has the more unusual fourfold square-planar oxygen coordination. The fact that Li2 is situated slightly above or below the oxygen plane is probably because of the long distance to the neighbours in those directions. The fact that the V_6O_{13} host structure remains centrosymmetric can be explained by the large distances between Li2 and its second-nearest neighbours. From the refinement of Li2 as two separate, equally occupied sites on either side of the single layer, it was concluded that the Li2—O5 and Li2—O6 distances are both greater than 3.1 Å.

The refined $Li_{3.24}V_6O_{13}$ structure is surprisingly similar to $Li_3V_6O_{13}$. Comparing V—O bond lengths, the largest difference is 0.015 (2) Å (V2—O7) with an average difference of 0.005 (4) Å. Thus, at this level of occupancy, the new lithium ion clearly has no major influence on the electronic structure of the host material. The oxygen coordination around Li3 resembles that of Li1, with five O atoms forming a square-pyramidal arrangement, with O2 and O5 forming the base and O6 the apex of the pyramid. As for Li1, the square base of the Li3 coordination pyramid is somewhat distorted. The refined occupancy gives a net composition of $Li_{3.24}V_6O_{13}$, slightly lower than the expected value from the discharge curve, but still reasonable. The refinement of Li3 shows that it enters the structure as a solid solution, *i.e.* it shows no observable preference for the different equivalent sites.

4.2. Lithium insertion mechanism in $Li_xV_6O_{13}$, $3 < x < 6$

The following discussion of the lithium insertion mechanism for $Li_xV_6O_{13}$, $3 < x < 6$, is based on the structures above and the shape of the discharge curve for V_6O_{13} *versus* Li/Li^+ in the region of interest. It is speculative but gives a reasonable explanation for the observations made. In the discussion (I) and (II), and *A*, *B*, *C* and *D* will refer to the notation used in Fig. 3.

As discussed above, Li2 is randomly disordered in both $Li_3V_6O_{13}$ and $Li_{3.24}V_6O_{13}$, while Li3 shows typical solid solution behaviour. Fig. 3 shows Li2 to be situated in one of two possible 'channels', (I) and (II) in the structure; in this case

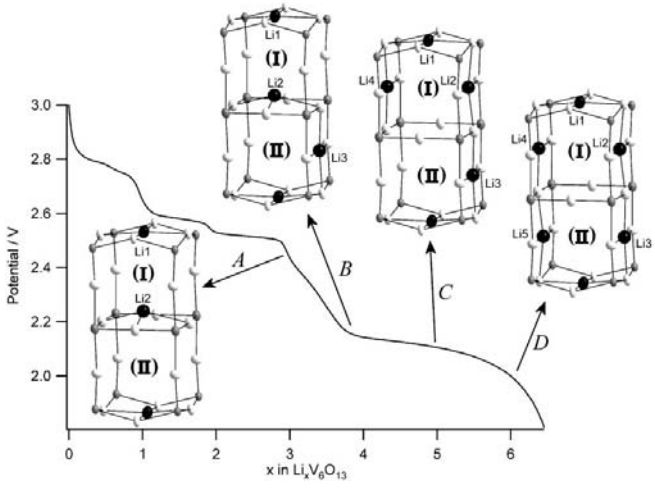

Figure 3
Proposed lithium insertion mechanism in a two-channel system: (I) and (II) label the two channels; *A*, *B*, *C* and *D* show the lithium positions at different stages of the insertion process. White, grey and black atoms are oxygen, vanadium and lithium, respectively.

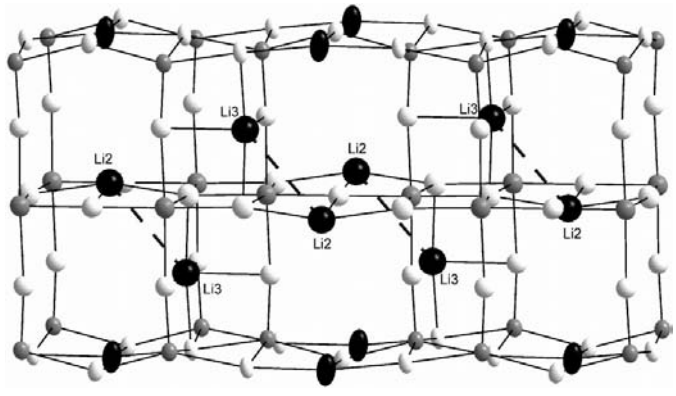

Figure 4
Schematic figure showing the short-range-order lithium insertion mechanism for Li3 in $Li_3V_6O_{13}$, governed by the randomly disordered Li2. Dashed lines link Li2/Li3 pairs; the positions of Li2 have been chosen arbitrarily. White, grey and black atoms are oxygen, vanadium and lithium, respectively.

[1] Supplementary data for this paper are available from the IUCr electronic archives (Reference: BM5009). Services for accessing these data are described at the back of the journal.

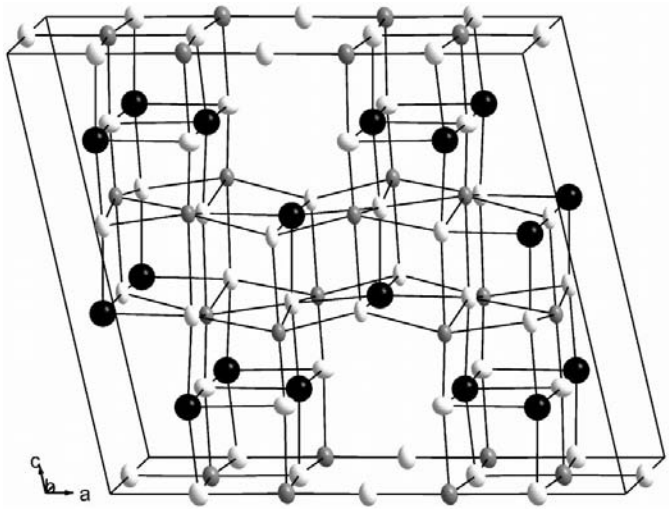

Figure 5
A proposed structure for $Li_6V_6O_{13}$. White, grey and black atoms are oxygen, vanadium and lithium, respectively.

arbitrarily chosen to occupy (I)*A*. When Li3 enters the structure, it has two possible sites to choose between, above or below the single layer. The site chosen depends on the position of Li2; the distance between the Li2 and Li3 site on the same side of the double layer is less than 2.6 Å. Electrostatic repulsion will thus force Li3 to enter (II)*B*. Furthermore, since Li2 is randomly disordered, as is Li3. A schematic representation of this behaviour is given in Fig. 4. This mechanism, whereby the position of Li3 is totally correlated to that of the disordered Li2, prevails until the net composition of the cathode reaches $Li_4V_6O_{13}$. At this point, all available Li3 sites are filled and lithium (let us call it Li4) will start to be inserted into (I). The insertion of Li4 into the structure and its impact (or lack of impact) on the discharge curve is reflected in the discharge curve for V_6O_{13} *versus* Li/Li^+ (Fig. 3); the potential is seen to drop rapidly between $x = 3$ and 4, before assuming a gradual slope over the composition range $4 < x < 6$, after which the potential again falls rapidly. This suggests that a new phase is formed at $x = 4$ and that two-phase equilibrium is maintained up to the composition $Li_6V_6O_{13}$. As Li4 begins to enter (I), it comes very close to Li2, whereupon electrostatic repulsion forces Li2 to move to a new site. The obvious candidate is clearly between the V1 and V3 octahedra, since such a site closely resembles those for Li1 and Li3. It is unlikely that Li2 would pass through the single layer, but probably moves to the site exactly opposite Li4 (*C*). There is now only one free lithium position left in (II) in the two-channel system (*C*). From this situation, there are two possible mechanisms for achieving $Li_6V_6O_{13}$; either the last free lithium site in (II) becomes occupied to form $Li_6V_6O_{13}$ (*D*) or *C* is formed throughout the structure before *D* is formed. From the shape of the discharge curve, the formation of *D* is the more plausible; *C* is thus a short-lived 'transition-phase' between *B* and *D*. The probable reason for this behaviour is that it is energetically more favourable to fill the last vacant lithium site than to force another Li2 into a new position. When the last lithium site in (II) becomes occupied (*D*), the cathode composition is $Li_6V_6O_{13}$; a proposed structure for this phase is given in Fig. 5.

5. Conclusions

A reinvestigation of $Li_3V_6O_{13}$, using area-detector data, finds no superstructure reflections and thus confirms that Li2 is indeed disordered in an otherwise centrosymmetric $Li_xV_6O_{13}$ host structure. On inserting additional lithium to form $Li_{3+\delta}V_6O_{13}$, $\delta \leq 1$, the newly inserted ion (Li3) is itself disordered, but its position is highly correlated with that of Li2. The apparent solid solution in the range $3 < x < 4$ is thus a direct result of the random disorder of Li2.

This work has been supported by The Swedish Science Council (VR) and The Swedish Energy Agency (STEM). We also wish to thank Yngve Cerenius at MAX-lab for his technical assistance during the measurements at I711.

References

Aebi, F. v. (1948). *Helv. Chim. Acta*, **31**, 8–21.
Berghoff, G. (1996). *DIAMOND*, Version 2.1c. Visual Crystal Information System, Bonn, Germany.
Bergström, Ö., Gustafsson, T. & Thomas, J. O. (1997). *Acta Cryst.* C**53**, 528–530.
Bergström, Ö., Gustafsson, T. & Thomas, J. O. (1998). *Acta Cryst.* C**54**, 1204–1206.
Björk, H., Lidin, S., Gustafsson, T. & Thomas, J. O. (2001). *Acta Cryst.* B**57**, 759–765.
Bruker (2003). *SMART* (Version 5.611), *SAINT*+ (Version 6.45), *SADABS* and *XPREP*. Bruker AXS Inc., Madison, Wisconsin, USA.
Ceder, G. & Aydinol M. K. (1998). *Solid State Ion.* **109**, 151–157.
Cerenius, Y., Ståhl, K., Svensson, L. A., Ursby, T., Oskarsson, Å., Albertsson, J. & Liljas, A. (2000). *J. Synchrotron Rad.* **7**, 203–208.
Gustafsson, T., Thomas, J. O., Koksbang, R. & Farrington, G. C. (1992). *Electrochim. Acta*, **37**, 1639–1643.
Lampe-Önnerud, C. & Thomas, J. O. (1995). *Eur. J. Solid State Inorg. Chem.* **32**, 293–302.
Petricek, V. & Dusek, M. (2000). *JANA*2000. Institute of Physics, Prague, Czech Republic.
Saeki, M., Kimizuka, N., Ishii, M., Kawada, I., Nakano, M., Ichinose, A. & Nakahira, M. (1973). *J. Crystal Growth*, **18**, 101–102.
Wilhelmi, K. A., Waltersson, K. & Kihlborg, L. (1971). *Acta Chem. Scand.* **25**, 2675–2687.